

A comprehensive study of comet 67P/Churyumov-Gerasimenko in the 2021/2022 apparition

Oleksandra Ivanova^{1,2,3}, V. Rosenbush^{2,3}, I. Lukiyanuk^{3,4}, V. Kleshchonok^{3,4}, N. Kiselev⁵, L. Kolokolova⁶, J. Markkanen⁷, C. Snodgrass⁸, D. Gardener⁸, E. Shablovinskaya⁹

(1) Astronomical Institute of Slovak Academy of Sciences, Slovak Republic, e-mail: oivanova@ta3.sk; (2) Main Astronomical Observatory of National Academy of Sciences of Ukraine, Ukraine
(3) Astronomical Observatory of Taras Shevchenko National University of Kyiv, Ukraine; (4) Max Planck Institute for Solar System Research, Germany; (5) Crimean Astrophysical Observatory, Crimea;
(6) University of Maryland, USA; (7) Institut für Geophysik und Extraterrestrische Physik, Technische Universität Braunschweig, Germany; (8) Institute for Astronomy, The University of Edinburgh, Edinburgh, United Kingdom;
(9) Núcleo de Astronomía de la Facultad de Ingeniería, Universidad Diego Portales, Chile



OBSERVATIONS AND PROCESSING

1. Observations at the 6-m telescope. Quasi-simultaneous spectral, photometric, and polarimetric observations of comet 67P/C-G were carried out at the 6-m BTA SAO telescope with the focal reducer SCORPIO-2 on 2021 October 6 (–31 days before perihelion) and 2022 February 6 (+96 days after perihelion). The observations were performed with a CCD detector E2V CCD261-84 of 2048×4104 pixels and the 15×15- μm pixel size. The full field of view of the CCD chip is 6.8'×6.8' with an image scale of 0.4 arcsec/px. The twilight sky was observed to define flat-field corrections of the photometric and polarimetric images. To increase the signal-to-noise (S/N) ratio of the measured signal, on-chip binning 2×2 was applied to all observed images in the photometric and polarimetric modes, and binning 1×2 in the long-slit mode. The observational circumstances of observations are listed in Table 1. It contains the observation time (mid-cycle time, UT), heliocentric (r) and geocentric (Δ) distances, phase angle of the comet (α), position angle (φ) of the scattering plane, filter or grating, total exposure time (T_{exp}), number of observation cycles (N), and mode of observations.

Table 1. Log of observations of comet 67P/C-G at the 6-m telescope.

Date, UT	r , au	Δ , au	α , deg	φ , deg	Filter/grating	T_{exp} , s	N	Mode
2021 Oct 6	1.254	0.475	47.9	266.7	g, r-sdss	20,10	5,5	Ima
2021 Oct 6	1.254	0.475	47.9	266.7	R	30	16	ImaPol
2021 Oct 6	1.254	0.475	47.9	266.7	VPHG1200@540	60300	5	Sp
2022 Feb 6	1.675	0.709	10.5	133.5	CN, BC, RC	240, 300, 40	3,3,3	Sp
2022 Feb 6	1.675	0.709	10.5	133.5	r-sdss	15	15	ImaPol
2022 Feb 6	1.675	0.709	10.5	133.5	VPHG1200@540	300	6	Sp

2. Imaging photometry at the Liverpool telescope. For studying the morphology of the coma and some characteristics of dust in comet 67P/C-G, we used photometric observations from the robotic 2-m Liverpool Telescope (LT) also. The data were calibrated through a custom-built automated pipeline, described in detail by Gardener et al. (2022). The observational circumstances of the LT observations are listed in Table 2. It contains the observation time (mid-cycle time, UT), heliocentric (r) and geocentric (Δ) distances, phase angle of the comet (α), position angle (φ) of the scattering plane, filter or grating, total exposure time (T_{exp}), number of observation cycles (N), and mode of observations.

Table 2. Log of observations of comet 67P/C-G at the 2-m Liverpool telescope.

Date, UT	r , au	Δ , au	α , deg	φ , deg	Filter	T_{exp} , s	N
2021 Oct 9.138	1.247	0.468	48.2	267.5	r-sdss	20	5
2022 Feb 6.068	1.676	0.710	10.5	133.3	r-sdss	20	5
2022 Feb 7.989	1.675	0.709	10.5	133.5	r-sdss	20	5

SPECTRA OF COMET

The spectra of comet 67P/C-G obtained on 2021 October 6 and 2022 February 6 consist of the strong continuum formed by the scattering of the solar light on dust grains and emission spectrum. Fig. 1 shows the stages of the reduction of the cometary spectrum. To separate the continuum signal from the gaseous emissions, we used the high-resolution solar spectrum by Neckel & Labs (1984). Strong CN and relatively weak C_2 , C_3 , and NH_2 emissions are identified in the spectra of the comet. On 2021 October 6, the normalized reflectance gradient averages (15.2 ± 4.1) %/1000 \AA in the spectral range $\lambda 4450$ –6839 \AA , and on 2022 February 6, it is (14.2 ± 0.4) %/1000 \AA in this range. The production rate ratio $\log(Q(C_2)/Q(CN))$ is -0.2 ± 0.4 for 2021, and -0.6 ± 0.1 for 2022.

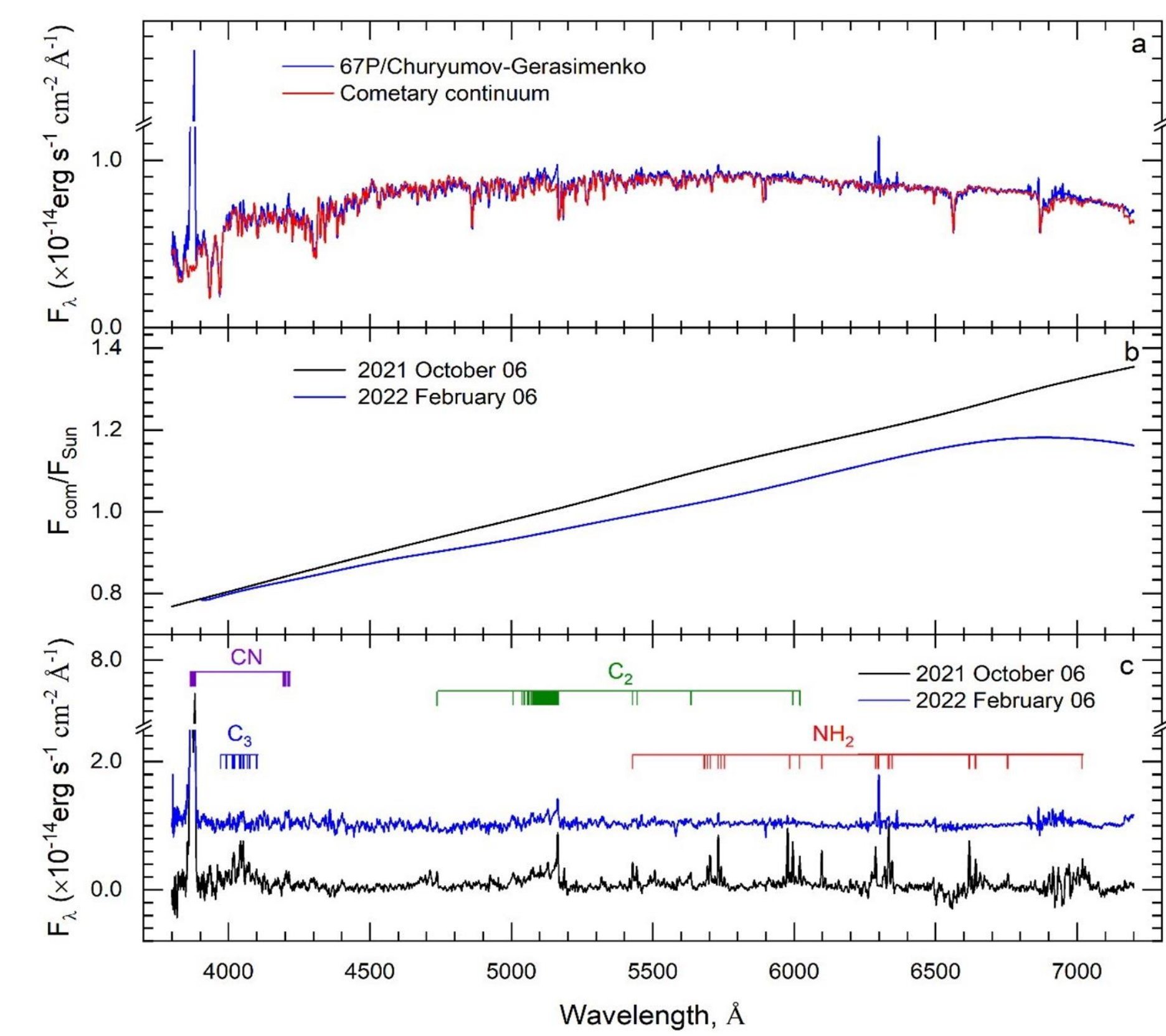


Figure 1. Reduction of the spectra of comet 67P/C-G obtained on 2021 October 6 and 2022 February 6. Panel (a) shows the spectrum of the comet (blue line) for 2021 October 6 with the scaled solar spectrum (red line); (b) is the normalized spectral dependence of the dust reflectivity; (c) shows two shifted emission spectra of the comet for the different dates of observations.

MORPHOLOGY OF THE DUST COMA

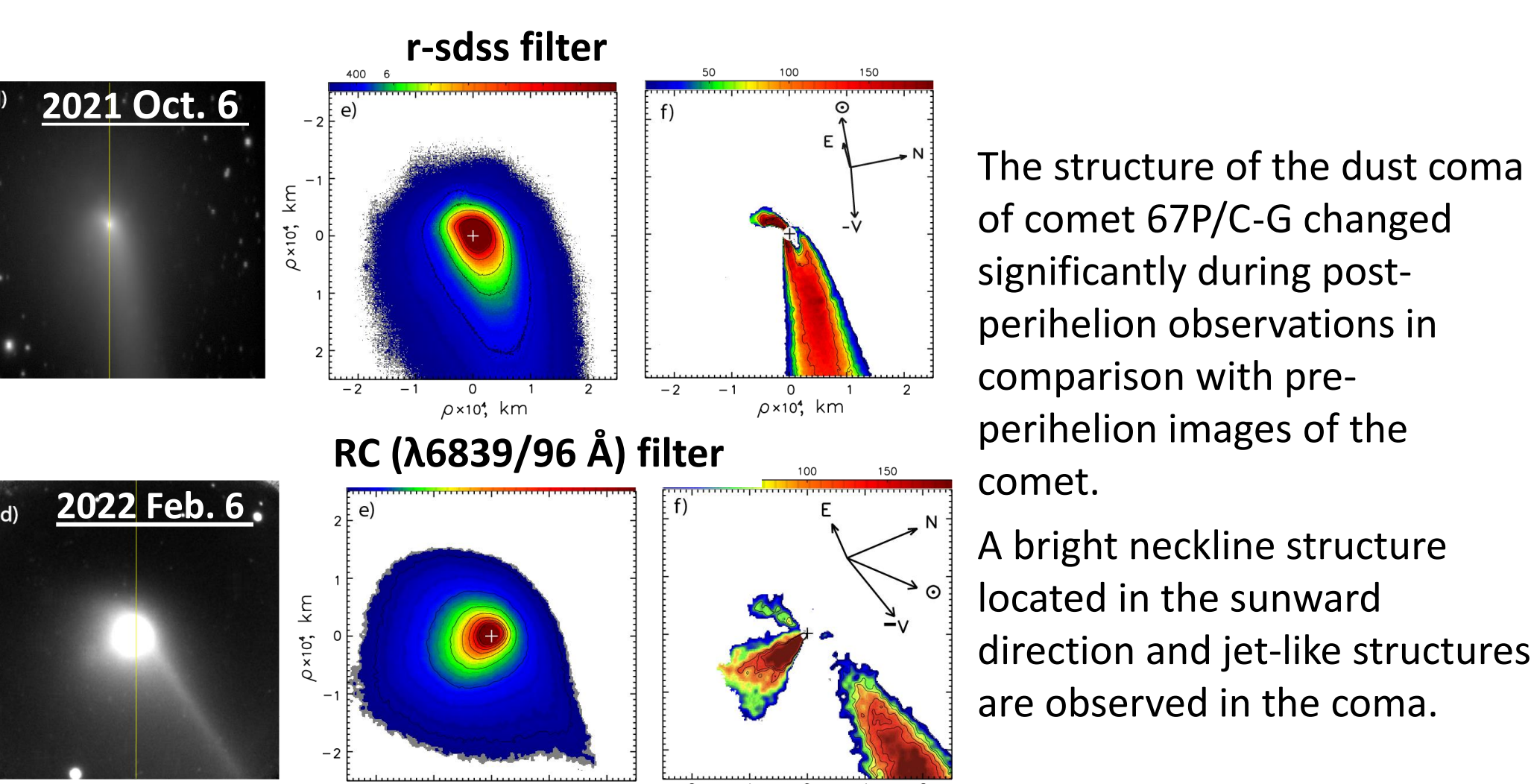


Figure 2. Images of comet 67P/C-G observed at the 6-m telescope. Panel (d) is the original CCD image of the comet and the position of the slit (yellow line) during spectral observations; (e) is the image with relative isophotes; (f) is the image to which a rotational gradient technique of Larson & Sekanina (1984) is applied.

INTRODUCTION

Comet 67P/Churyumov-Gerasimenko (67P/C-G hereafter) is a Jupiter family comet with an orbital period of about 6.44 years. In the previous apparition, the comet was intensively studied by the European Space Agency's Rosetta rendezvous mission during 2014–2016 and a worldwide ground-based campaign and thus is one of the best-studied comets. In that apparition, within the framework of the ground-based support of the Rosetta mission, we carried out extensive observations of comet 67P/C-G in the post-perihelion period from 2015 November to 2016 April using the 6-m BTA SAO telescope. The results of these observations provided valuable insight into the coma processes beyond Rosetta's coverage (Ivanova et al. 2017; Rosenbush et al. 2017; Snodgrass et al. 2017). One of the main objectives of our investigation of comet 67P/C-G in the recent 2021/22 apparition was to make the same comprehensive observations with the same telescope and directly compare the results obtained for dust and gas components of the cometary coma to those taken during the 2015/16 apparition. The comet passed its last perihelion on 2021 November 2.1 UT at a heliocentric distance of 1.211 au. In this apparition, the comet was at the closest approach to Earth since 1982: the minimum geocentric distance was 0.418 au on 2021 November 11. We conducted two pre- and post-perihelion sets of quasi-simultaneous photometric, spectroscopic, and polarimetric observations using different telescopes. Our work focuses on studying the optical and physical properties of gas and dust components of comet 67P/C-G using spectra, coma morphology, and colour and polarimetric maps, as well as modelling light scattering by dust particles.

PHOTOMETRY OF THE COMET

1. Morphology of dust and gas coma. To better understand the dust and gas environment of comet 67P/C-G, we observed it using the 6-m telescope on 2021 October 6 (31 days before perihelion) with g-sdss and r-sdss filters, and on 2022 February 6 (96 days after perihelion) with narrowband HB filters: BC, RC, and CN. We used the r-sdss, BC, and RC filters to analyze dust and applied a rotational gradient technique to enhance contrast and reveal subtle morphological details in the comet that aren't visible in unprocessed images (Fig. 3).

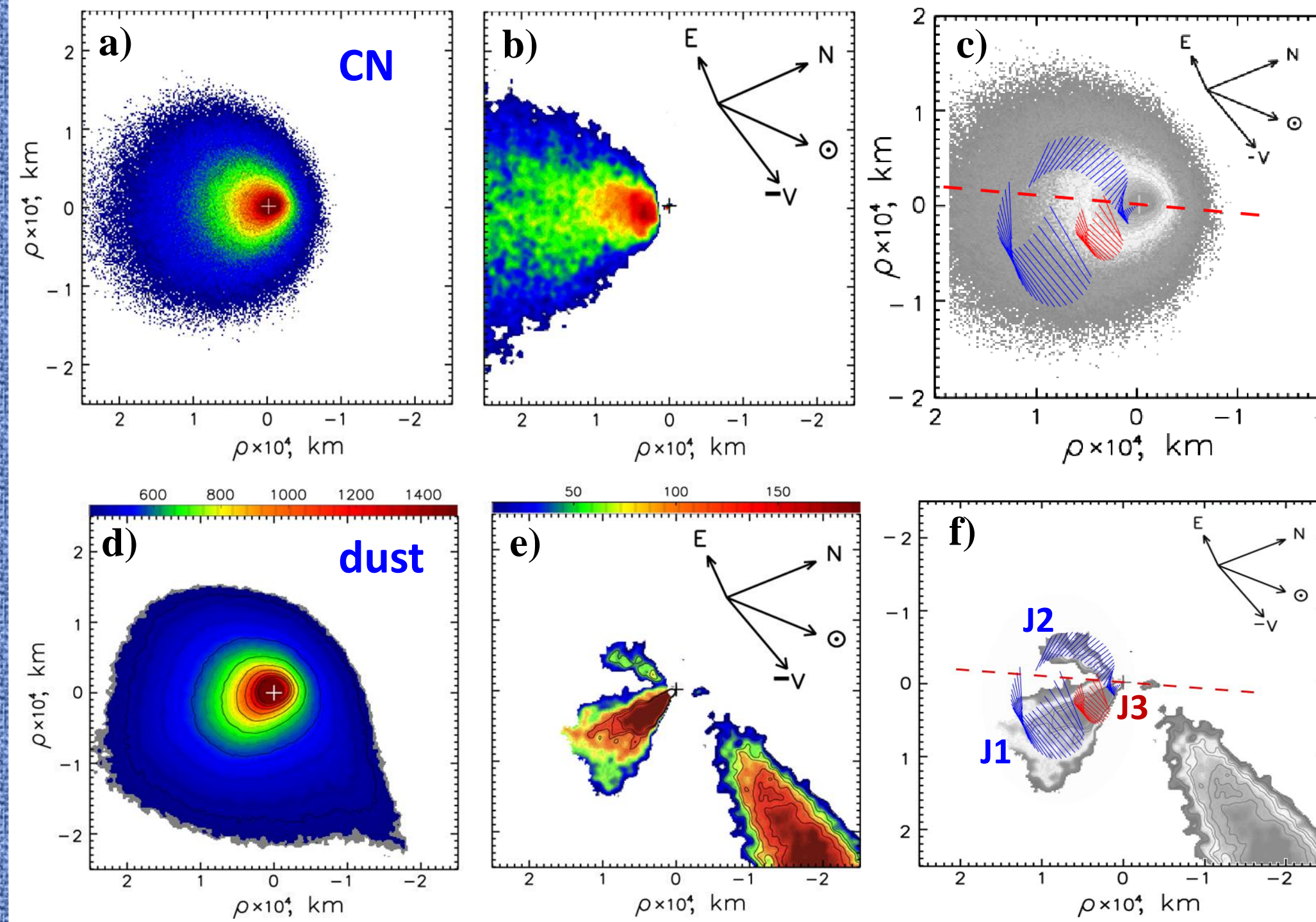


Figure 3. Co-added images of comet 67P/C-G observed at the 6-m telescope with the narrowband cometary filters CN and RC. Panels (a) and (d) are the images with relative isophotes differing by a factor of $\sqrt{2}$ in intensity; (b) and (e) are the images to which a rotational gradient technique of Larson & Sekanina (1984) is applied. Panels (c) and (f) show the formation of CN coma and jets from the nucleus using the geometric model.

On 2021 October 6, the sunward jet and long dust tail are detected in the images of the comet (Fig. 2). The structure of the dust coma of the comet changed significantly after perihelion on February 6, 2022. The most prominent feature is the bright neck-line structure in the direction of the Sun (Fig. 2). The enhanced images showed two jets which are located symmetrically relative to the rotation axis of the nucleus. Using a geometric model, we found that two observed jets are formed from the same active area located at a latitude of $\varphi = -58^\circ \pm 5^\circ$ and the opening angle $26^\circ \pm 8^\circ$. Jet J3 is formed from the other active area, $\varphi = -53^\circ \pm 10^\circ$, which is separated from the first one by a difference in longitude of $150^\circ \pm 20^\circ$. We detected the unusual morphology of the CN coma and showed that there is an additional source of CN radical originating from dust jets.

2. Dust production rate and normalized reflectivity gradient of the dust. The maximum value of $Afp \approx 290$ cm, obtained in an aperture with a radius of 2000 km (Fig. 4), exactly corresponds to the position of Afp on the linear fitting curve at a heliocentric distance of $r = 1.25$ au based on all available data for 1982, 1996, 2002, 2009, and 2015 apparitions of comet 67P/C-G (see Figure 6, Ivanova et al. 2017).

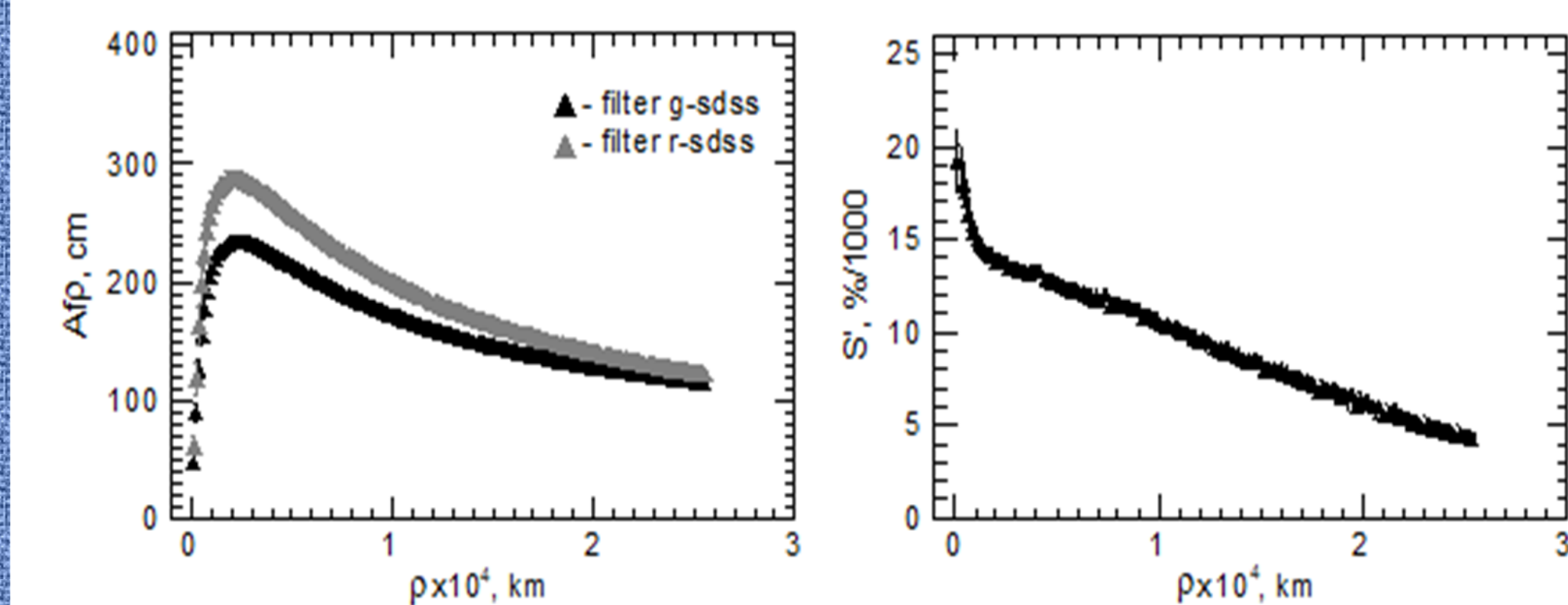


Figure 4. Afp profiles taken in the g-sdss and r-sdss filters as observed in comet 67P/C-G 2021 October 6 (left panel). The right panel shows a change in the normalized spectral gradient of the reflectivity S' with cometary distance ρ within the g-r domain at the same date.

3. Radial profiles of surface brightness

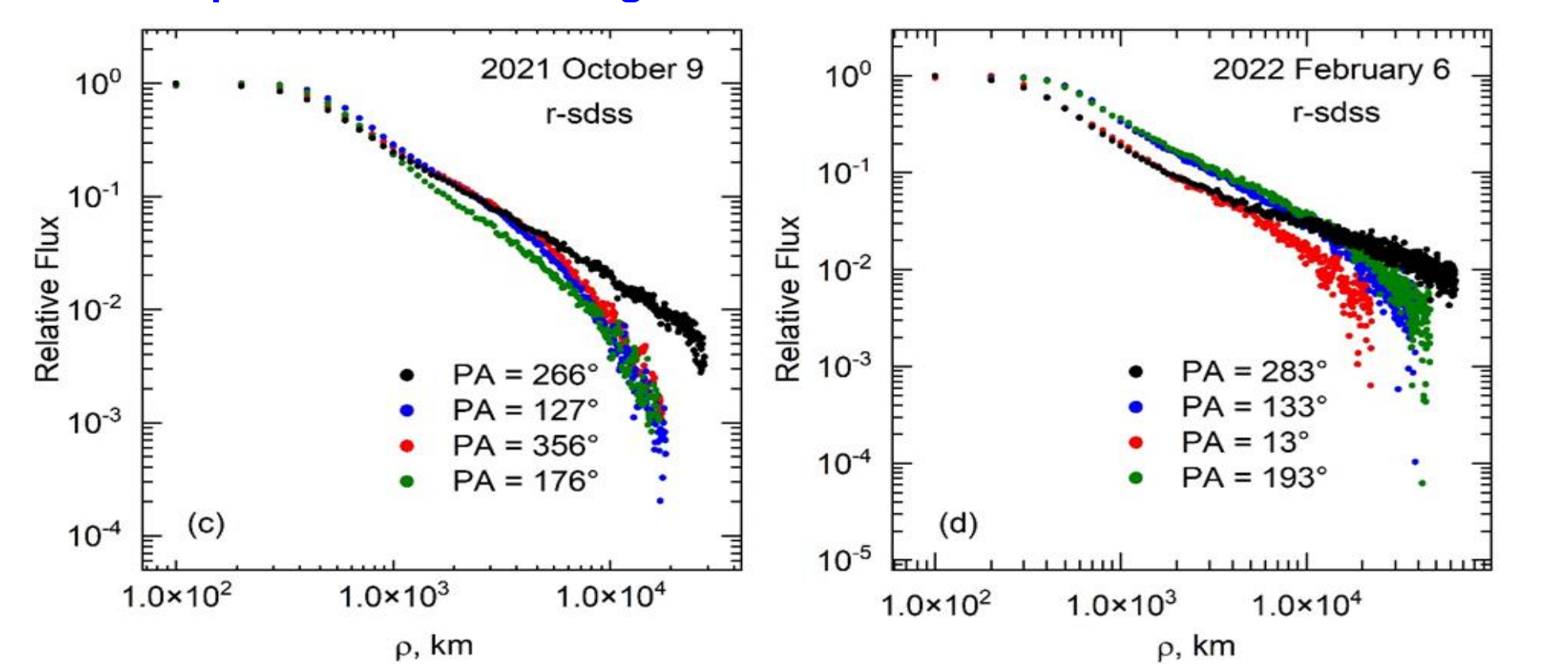


Figure 5. Radial profiles of the surface brightness of the dust coma of comet 67P/C-G as a function of projected cometary distance ρ obtained from the images taken in the r-sdss filters on 2021 October 9 (left panel) and on 2022 February 6 (right panel) at the LT telescope.

COLOUR AND POLARIMETRY MAPS

The colour and polarimetry maps are given in Fig. 6 and Fig. 7, respectively. The redder colour around the optocentre appears to be the result of seeing blurring of the nucleus region. The colour of dust in the jet and coma decreases quite sharply with the cometary distance, from ~ 0.7 – 0.8 mag near the nucleus to ~ 0.2 mag at the distance ~ 17 000–19 000 km. Contrary, the colour of the dust in the tail is very red, about 0.8 mag, and remains nearly unchanged up to distances of almost 40 000 km. Contrary, in 2022 February, at the phase angle $\alpha = 10.5^\circ$, the comet exhibits a more complex coma structure in polarized light: the polarization degree along the neckline smoothly decreases with distance from the nucleus from $\sim 1\%$ to $\sim 2\%$ at 45 000 km; almost the same polarization trend is observed along the two jets J1 ($PA=193^\circ$) and J2 ($PA=133^\circ$); in the coma, the polarization drops sharply from $\sim 1\%$ to $\sim 4\%$ at a distance of 20 000 km from the nucleus. In general, the polarization phase curve of comet 67P/C-G resembles that of a highly polarized dust comet, however, it seems that higher polarization values are observed specifically in the 2021/22 apparition.

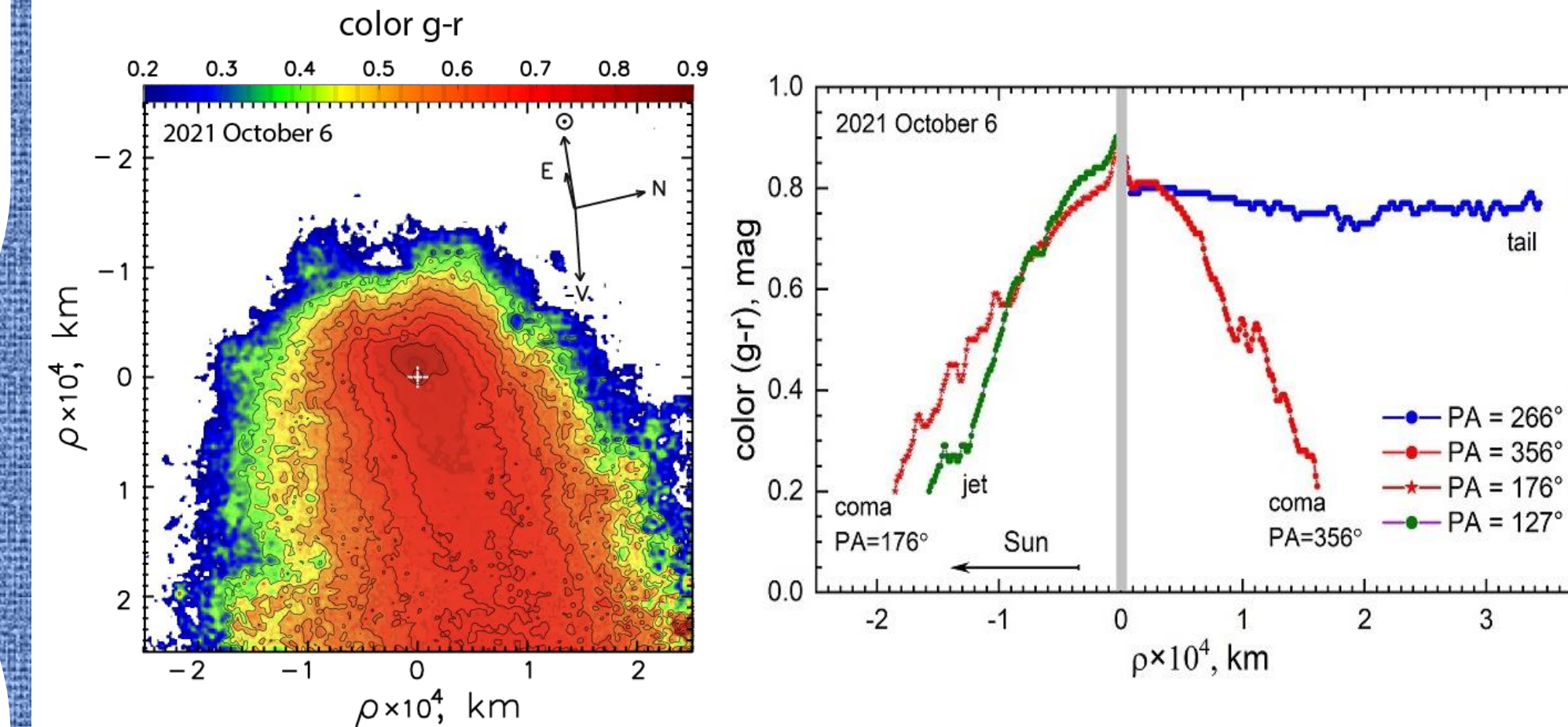


Figure 6. The left panel shows the (g-r) colour map of comet 67P/C-G acquired on 2021 October 6, and the right panel shows the colour scans in different directions.

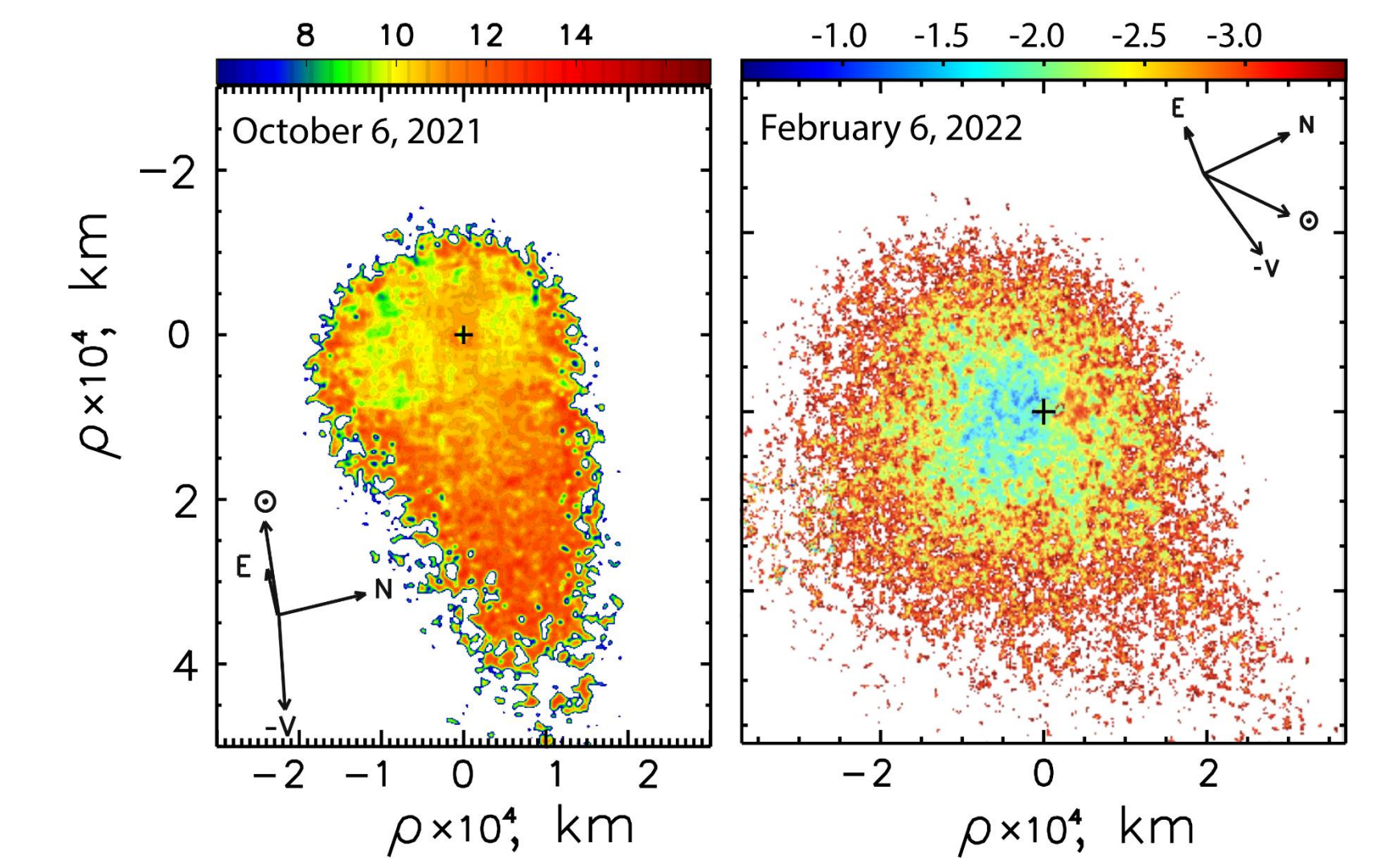


Figure 7. The left panel shows the linear polarization map taken on 2021 October in the R filter, and the right panel shows the linear polarization map taken on 2022 February in the r-sdss filter.

Aperture polarimetry. The phase-angle dependence of the degree of polarization of the comet 67P/C-G is displayed in Fig. 7. In general, the phase polarization curve of comet 67P/C-G resembles the curve for highly polarized dust comets.

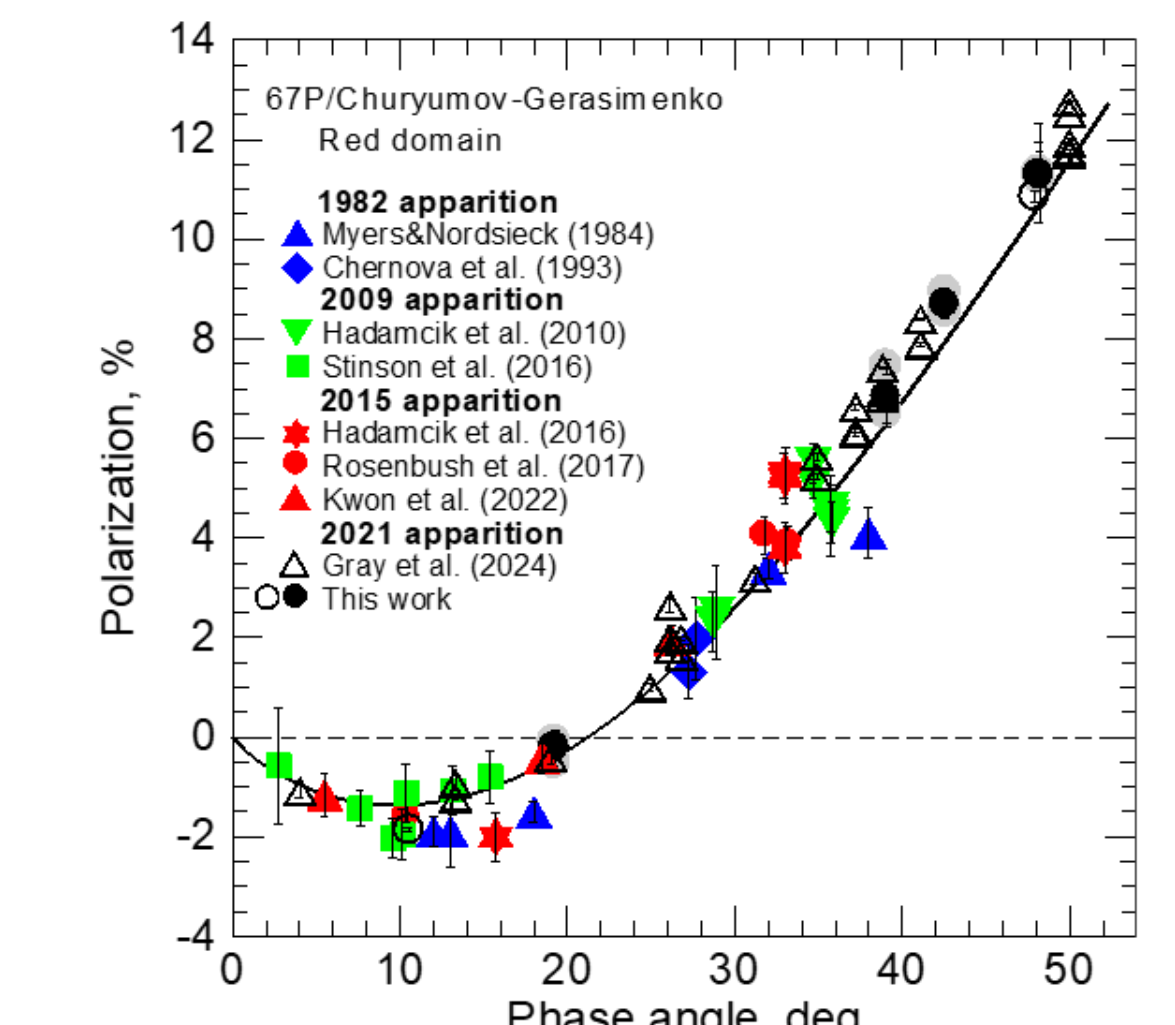


Figure 7. Polarization of comet 67P/C-G as a function of phase angle in different apparitions. The solid line shows the average phase-angle dependence of polarization for high-Pmax comets in the red continuum taken from (Kiselev et al. 2015).

PRELIMINARY NUMERICAL MODELLING OF COLOUR AND POLARIZATION

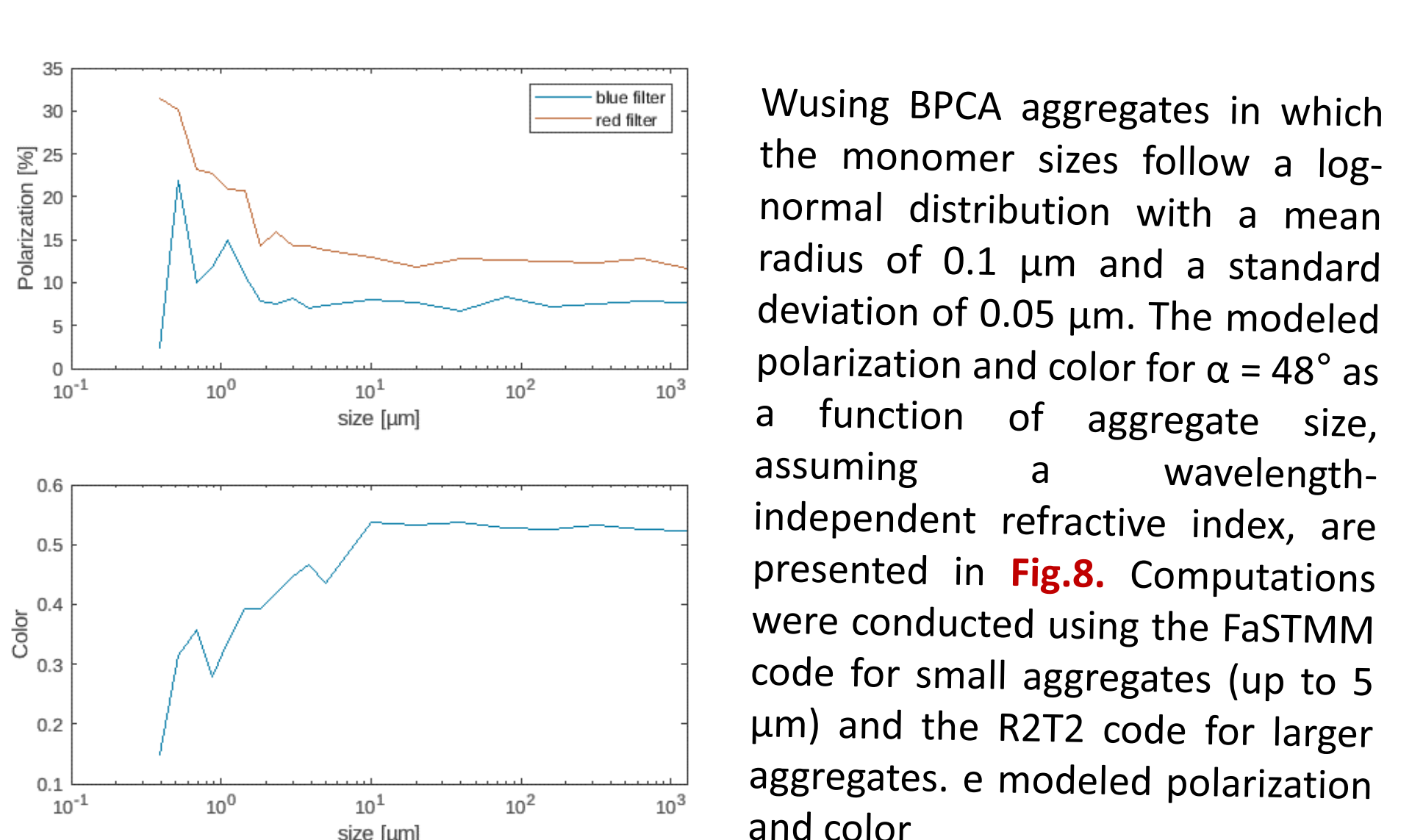


Figure 8. Modelled polarization and color for October 6. The modeling results are consistent with the dynamical sorting effect, where large particles populate the region near the nucleus and the tail, while small particles are dispersed throughout the coma due to higher initial velocities.

Acknowledgments

This work is supported by the Partnership Fund of the University of Edinburgh and Taras Shevchenko National University of Kyiv. The work by OI was supported by the Slovak Grant Agency for Science VEGA (Grant No. 2/0059/22) and by the Slovak Research and Development Agency under the Contract No. APVV-19-0072. The research by OI, IL, and VR is supported by Project No. 0122U001911 of the Ministry of Education and Science of Ukraine. The researches by OI, IL, VR and by VK is supported by Projects No. 0122U001911 and 0124U001304 of the Ministry of Education and Science of Ukraine, respectively.

